

Ultrasonic Imaging of Anisotropic Domains: Fluid filled cracks and seismic anisotropy

Bode Omoboya

Collaborators:

Emrah Pacal

J.J.S de Figueiredo

Nikolay Dyaur

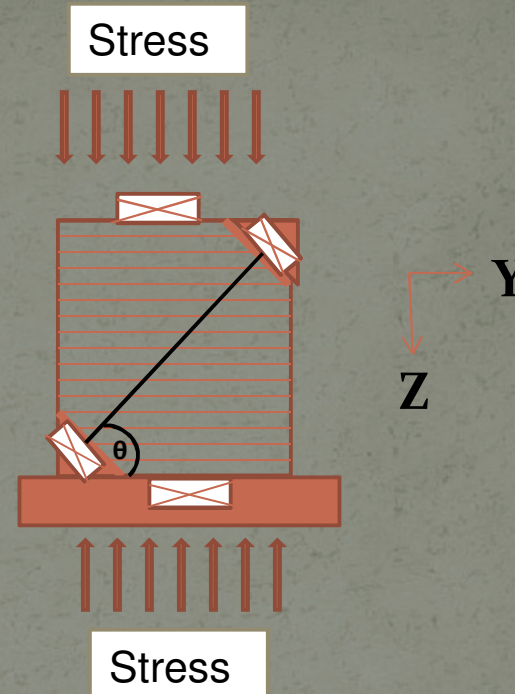
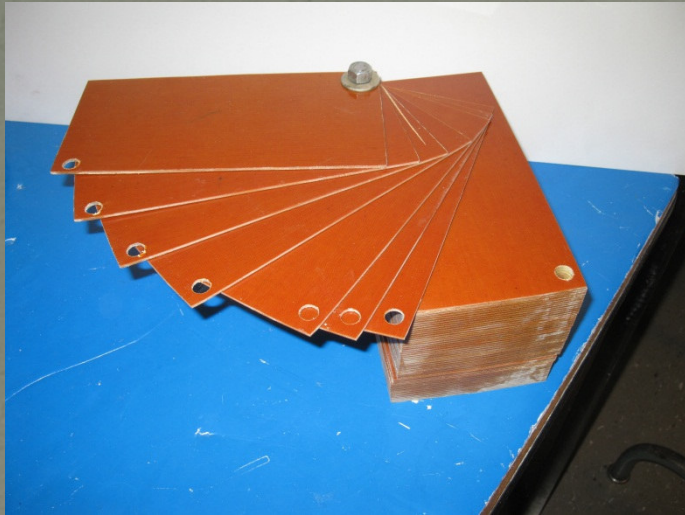
Robert. R Stewart



Outline

- Physical Modeling Examples
- Study Objectives
- Sample Description
- Experimental Methods
- Azimuthal P-Wave NMO results
- Travel time and Velocity results
- Stiffness coefficients and Anisotropic parameters
- Conclusion and Future work

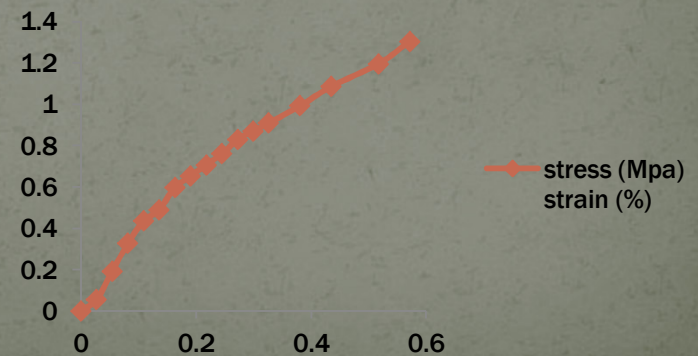
Physical Modeling Examples: Uniaxial Stress VS Anisotropy



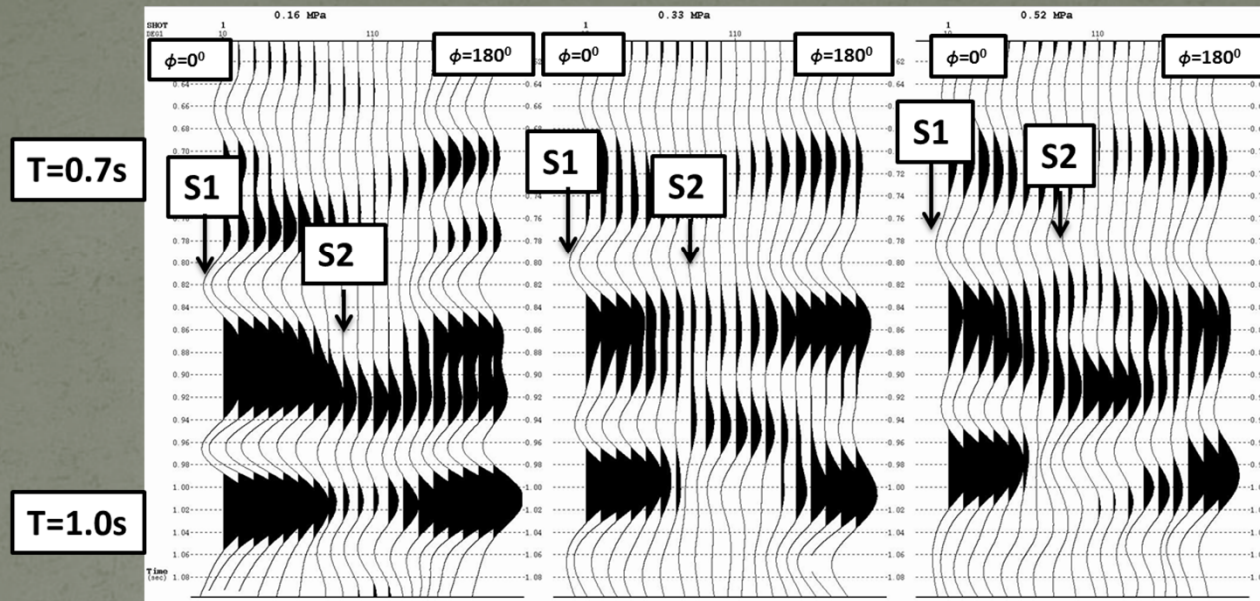
Uniaxial Stress and Ultrasonic Anisotropy in a Layered Orthorhombic Medium

Bode Omoboya
J.J.S de Figueiredo
Nikolay Dyaur
Robert. R. Stewart

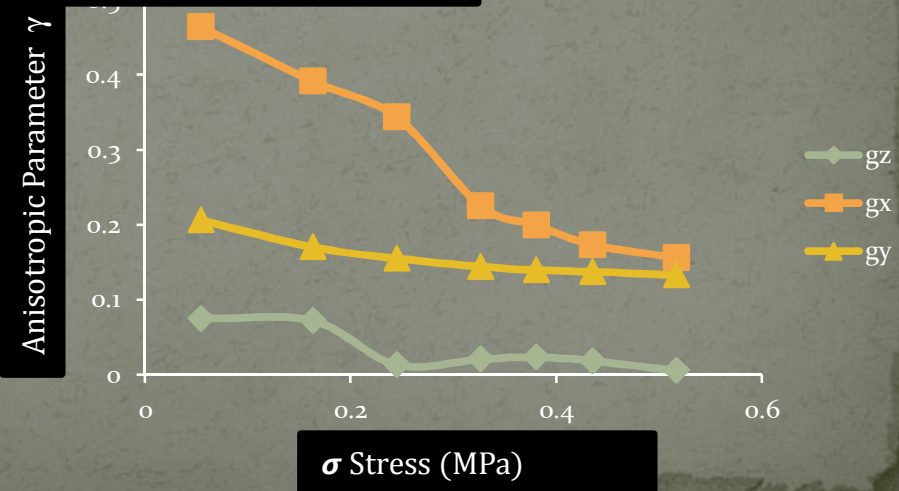
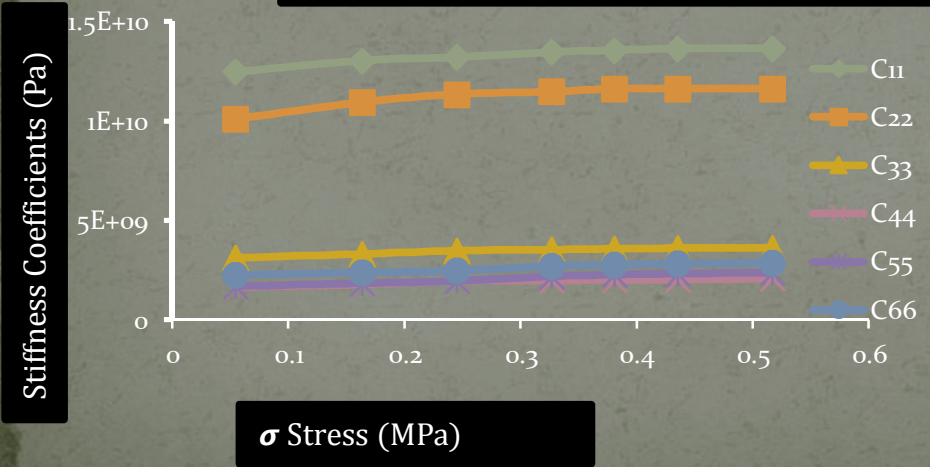
stress - strain curve



Physical Modeling Examples: Uniaxial Stress VS Anisotropy



Shear wave seismogram in different stress regimes
 a) 0.16MPa b) 0.36MPa c) 0.56MPa



Physical Modeling Examples: Source Frequency VS Anisotropy



$$\epsilon = \frac{N\pi r^2 h}{V}$$

Hudson, 1981

Model M₁
Reference Model

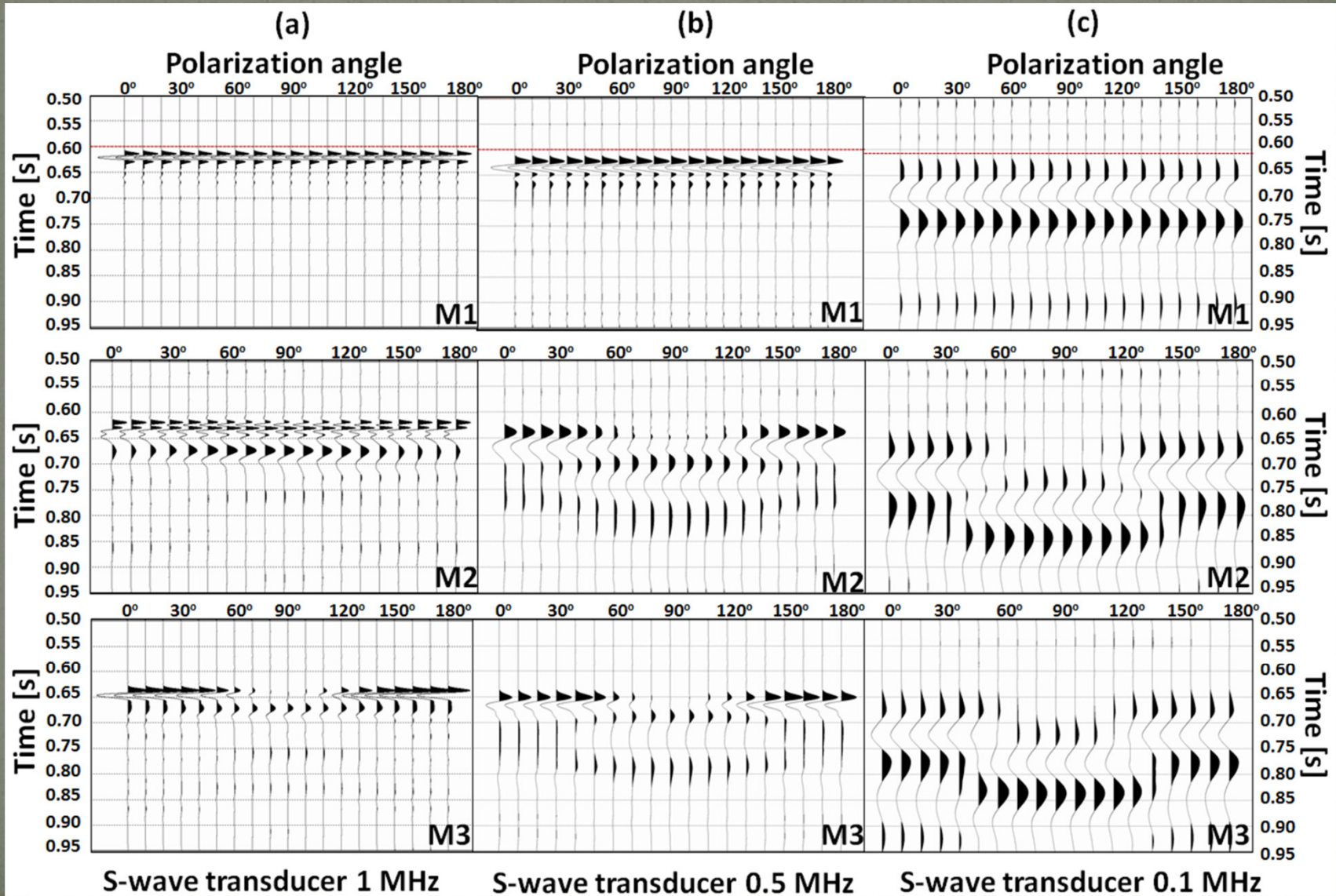
Model M₂
Crack Density = 4.5 %

Model M₃
Crack Density = 4.0 %

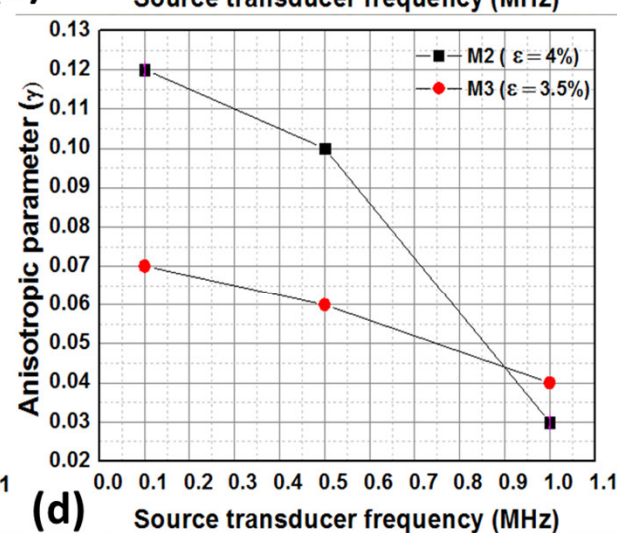
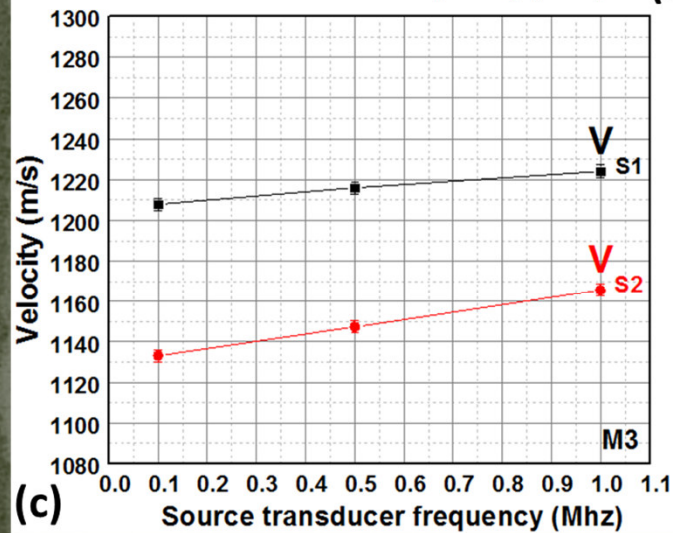
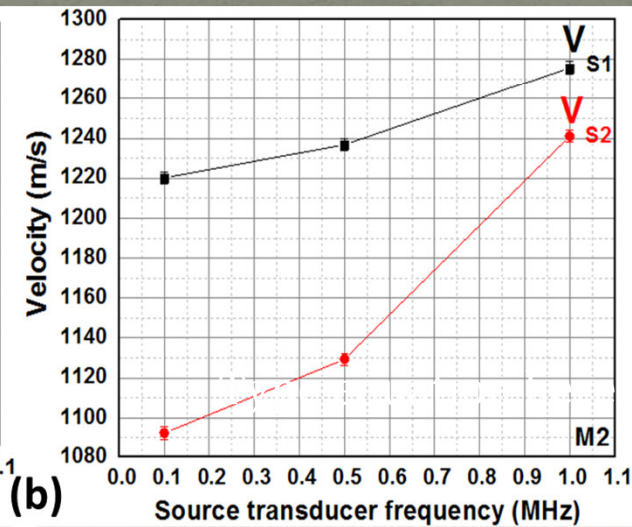
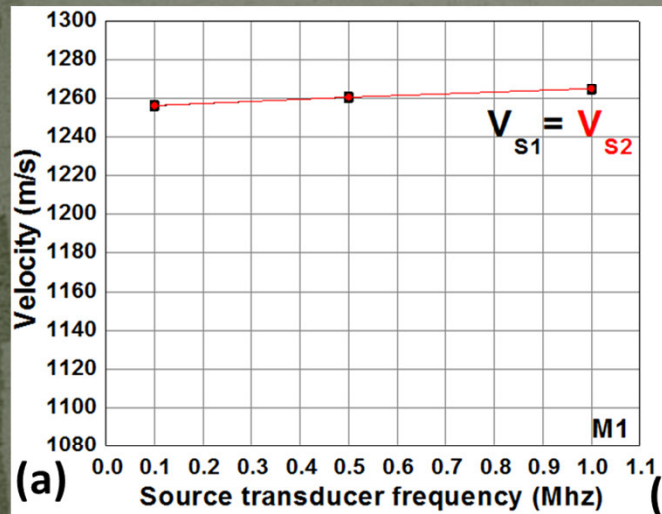
Effect of source frequency on seismic anisotropy

J.J.S de Figueiredo
Nikolay Dyaur
Bode Omoboya
Robert. R. Stewart

Physical Modeling Examples: Source Frequency VS Anisotropy



Physical Modeling Examples: Source Frequency VS Anisotropy



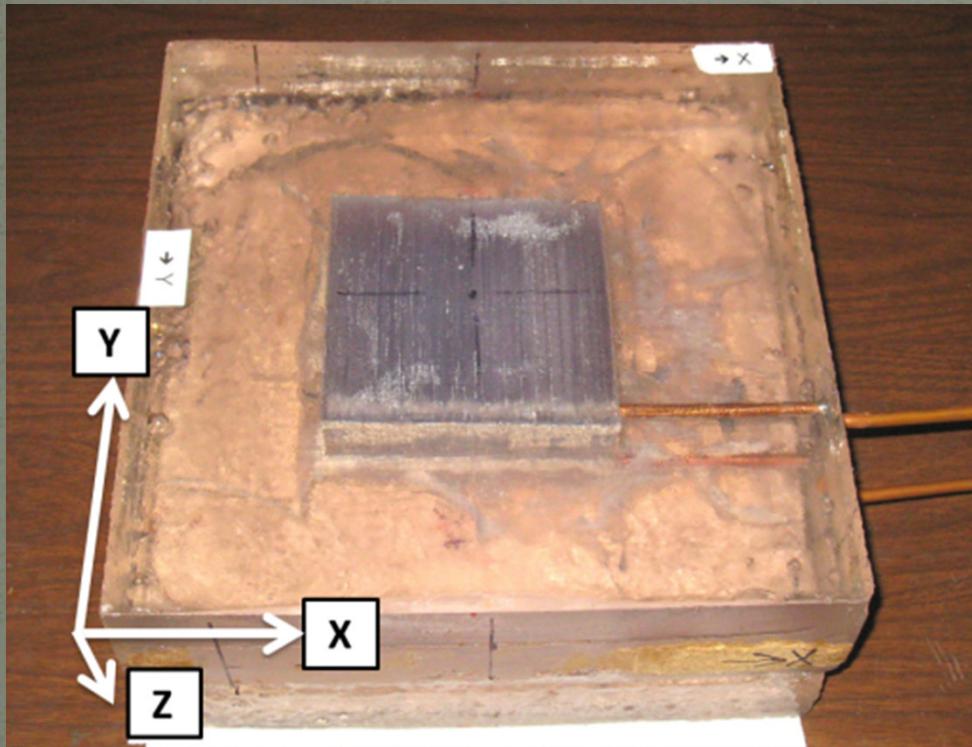
$$\gamma = \frac{1}{2} \left(\frac{V_{s1}^2}{V_{s2}^2} - 1 \right)$$

Thomsen, 1986

Study Objectives

- To explore the effect of different fluids on seismic response and consequently anisotropy in an inherently anisotropic medium.
- To compare predictions of various theories of wave propagation in fractured media to lab measurements.

Sample Description



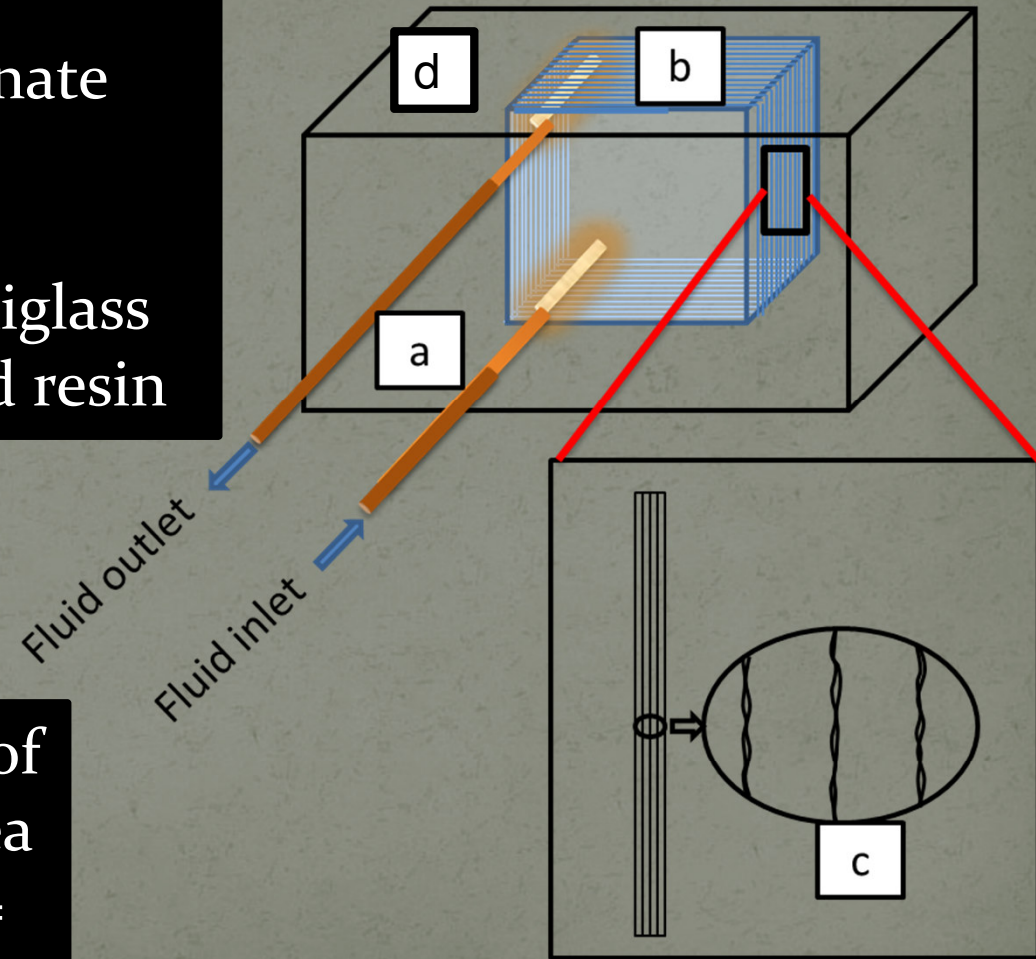
Constituent Materials:

- Resin
- Plexiglass (polycarbonate)
- Copper tubes

Model Dimensions = (296.9 X 296.7 X 131.6) mm

Sample Description – Schematic

- (a) Copper tubes
- (b) Plexiglass/polycarbonate stack
- (c) Grooves or scratches between stacked plexiglass
- (d) Isotropic background resin



Volume fraction/ratio of fractures plexiglass area to composite model =
0.12 : 0.88

Sample Description – Fractured area

- Fractured area is made up of 95 scratched plexiglass sheets each 1.1 mm to 1.3 mm thick
- Grooves or scratches on the sheets are 0.1 mm to 0.2 mm deep (on both sides)
- Fractures/scratches are randomly placed and run in all directions on the sheets
- Source-receiver transducers with dominant frequency 100kHz (dominant $\lambda \sim 30$ mm) was used in all experiments

Sample Description – Physical properties

Physical properties of Isotropic resin
(background medium)

$$V_p = 2540 \text{ m/s}$$

$$V_s = 1250 \text{ m/s}$$

$$\text{Density } \rho = 1.22 \text{ g/cc}$$

$$V_p/V_s = 2.032$$

$$\text{Poisson's ratio } \sigma = 0.340$$

$$\begin{pmatrix} \lambda + 2\mu & \lambda & \lambda & 0 & 0 & 0 \\ \lambda & \lambda + 2\mu & \lambda & 0 & 0 & 0 \\ \lambda & \lambda & \lambda + 2\mu & 0 & 0 & 0 \\ 0 & 0 & 0 & \mu & 0 & 0 \\ 0 & 0 & 0 & 0 & \mu & 0 \\ 0 & 0 & 0 & 0 & 0 & \mu \end{pmatrix}$$

Isotropic resin =

$$\begin{pmatrix} 7.79 \pm 0.05 & 4.04 \pm 0.1 & 4.04 \pm 0.1 & 0 & 0 & 0 \\ 4.04 \pm 0.1 & 7.79 \pm 0.05 & 4.04 \pm 0.1 & 0 & 0 & 0 \\ 4.04 \pm 0.1 & 4.04 \pm 0.1 & 7.79 \pm 0.05 & 0 & 0 & 0 \\ 0 & 0 & 0 & 1.87 \pm 0.06 & 0 & 0 \\ 0 & 0 & 0 & 0 & 1.87 \pm 0.06 & 0 \\ 0 & 0 & 0 & 0 & 0 & 1.87 \pm 0.06 \end{pmatrix}$$

GPa

Sample Description – Physical properties

Physical properties of scratched or fractured plexiglass stacks (cracked medium)

$$V_p \text{ (matrix)} = 2300 \text{ m/s}$$

$$V_s \text{ (matrix)} = 1320 \text{ m/s}$$

$$\text{Density (matrix)} \rho = 1.188 \text{ g/cc}$$

$$V_p/V_s \text{ (matrix)} = 1.742$$

$$\text{Poisson's ratio } \sigma \text{ (matrix)} = 0.254$$

$$\varepsilon = 0.35$$

$$\gamma = 0.39$$

$$\delta = 0.007$$

$$\text{Porosity } \phi = 2.5 \%$$

Estimated from travel time and anisotropic measurements (Thomsen, 1995)

$$\begin{pmatrix} C_{11} & C_{13} & C_{13} & 0 & 0 & 0 \\ C_{13} & C_{33} & (C_{33} - 2C_{44}) & 0 & 0 & 0 \\ C_{13} & (C_{33} - 2C_{44}) & C_{33} & 0 & 0 & 0 \\ 0 & 0 & 0 & C_{44} & 0 & 0 \\ 0 & 0 & 0 & 0 & C_{55} & 0 \\ 0 & 0 & 0 & 0 & 0 & C_{55} \end{pmatrix} =$$

$$\begin{aligned} \text{Crack density } \zeta &= 14 \% \\ \text{Crack aspect ratio } a &= 4.2 \% \end{aligned}$$

$$\begin{pmatrix} 5.01 \pm 0.1 & 1.56 \pm 0.31 & 1.56 \pm 0.31 & 0 & 0 & 0 \\ 1.56 \pm 0.31 & 1.73 \pm 0.05 & 1.25 \pm 0.1 & 0 & 0 & 0 \\ 1.56 \pm 0.31 & 1.25 \pm 0.1 & 1.73 \pm 0.05 & 0 & 0 & 0 \\ 0 & 0 & 0 & 0.24 \pm 0.02 & 0 & 0 \\ 0 & 0 & 0 & 0 & 0.09 \pm 0.01 & 0 \\ 0 & 0 & 0 & 0 & 0 & 0.09 \pm 0.01 \end{pmatrix} \text{ GPa}$$

Sample Description – Physical properties

Physical properties of whole sample/model
(composite medium)

$$\varepsilon = 0.22$$

$$\gamma = 0.21$$

$$\delta = 0.051$$

$$\text{Porosity } \phi = 2.5 \%$$

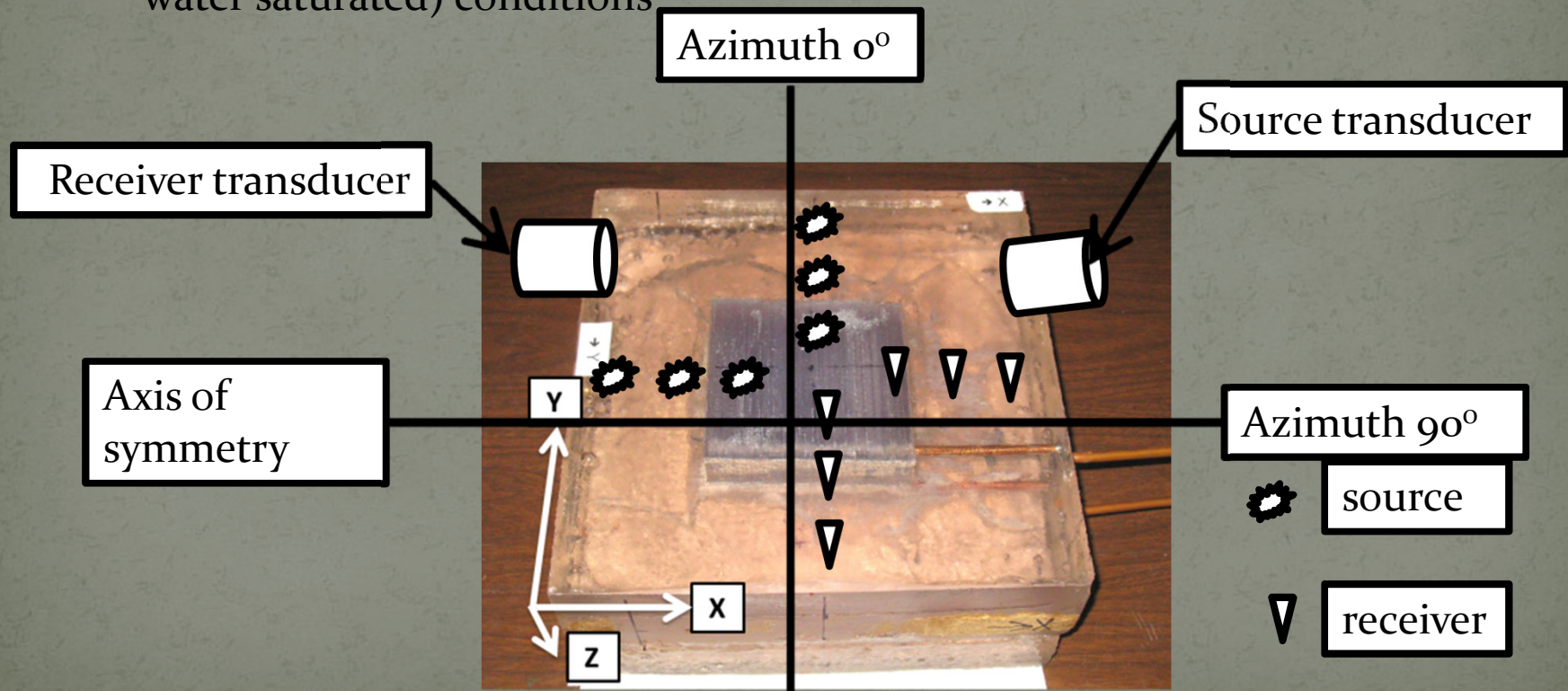
$$\begin{pmatrix} C_{11} & C_{13} & C_{13} & 0 & 0 & 0 \\ C_{13} & C_{33} & (C_{33} - 2 C_{44}) & 0 & 0 & 0 \\ C_{13} & (C_{33} - 2 C_{44}) & C_{33} & 0 & 0 & 0 \\ 0 & 0 & 0 & C_{44} & 0 & 0 \\ 0 & 0 & 0 & 0 & C_{55} & 0 \\ 0 & 0 & 0 & 0 & 0 & C_{55} \end{pmatrix} = \begin{pmatrix} 7.40 \pm 0.05 & 2.81 \pm 0.36 & 2.81 \pm 0.36 & 0 & 0 & 0 \\ 2.81 \pm 0.36 & 3.61 \pm 0.1 & 2.04 \pm 0.1 & 0 & 0 & 0 \\ 2.81 \pm 0.36 & 2.04 \pm 0.1 & 3.61 \pm 0.1 & 0 & 0 & 0 \\ 0 & 0 & 0 & 0.79 \pm 0.03 & 0 & 0 \\ 0 & 0 & 0 & 0 & 0.49 \pm 0.01 & 0 \\ 0 & 0 & 0 & 0 & 0 & 0.49 \pm 0.01 \end{pmatrix} \text{ GPa}$$

Sample Description - Summary

- ✓ Background resin medium was found to be isotropic and homogeneous.
- ✓ On close inspection, composite model was found to be slightly orthorhombic
 - ✓ $C_{11} \neq C_{22}$ or C_{33}
 - ✓ $C_{22} \approx C_{33}$ (5% difference but were treated as equal in our analysis)
- ✓ Fractured plexiglass inclusion zone has HTI symmetry
- ✓ Based on model fabrication setup and inverted parameters (Thomsen, 1995), we consider our cracks to be somewhat penny-shaped with very low aspect ratio (4.2%)
- ✓ In all measurements, source wavelength (λ) was 15 to 20 times greater than fracture aperture (H) $\{\lambda \gg H\}$

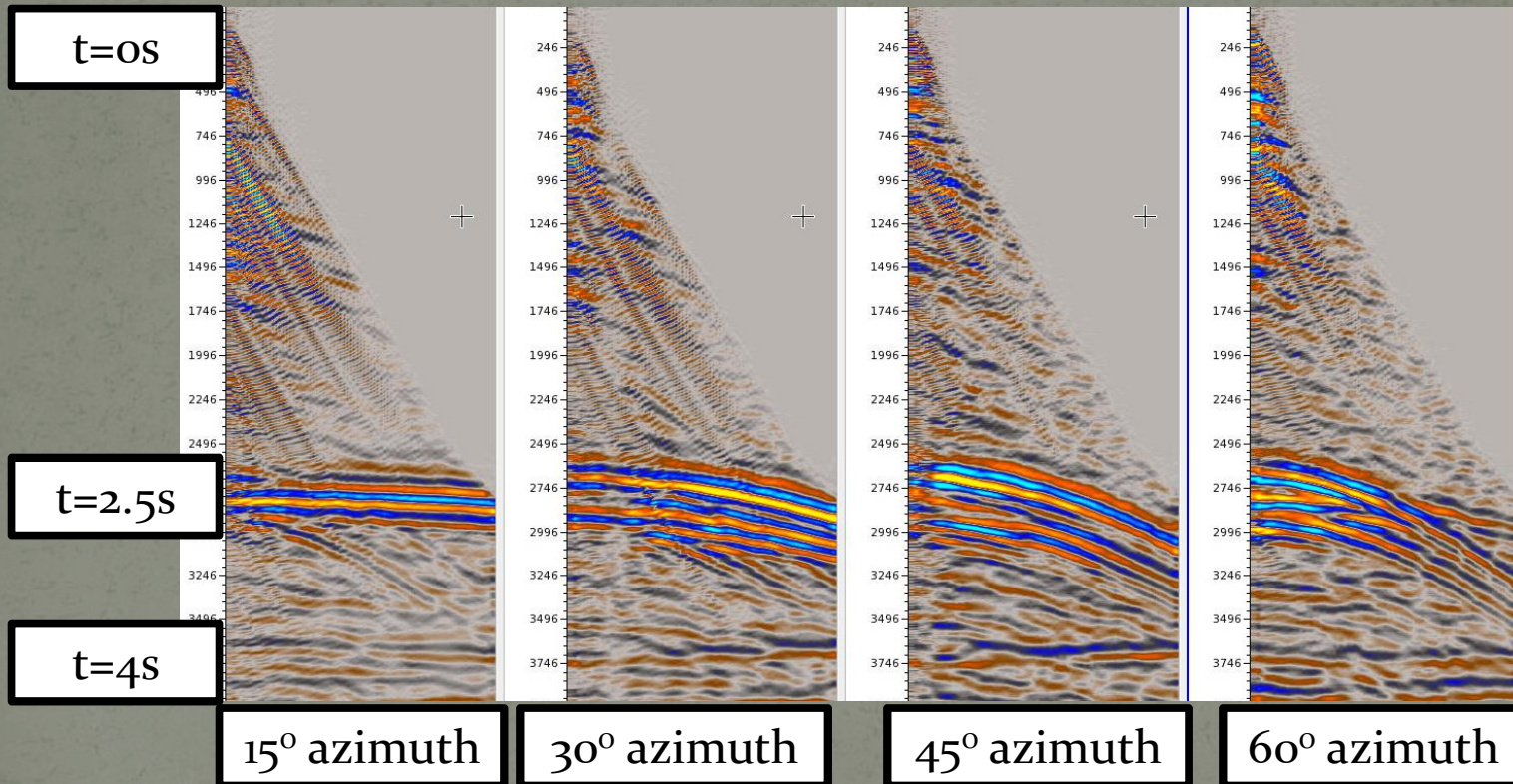
Experimental Methods

- Single source transmission measurements in all axes and directions at dry (Gas saturated), partially saturated (50% water saturation) and wet (100% water saturated) conditions
- Surface scaled CMP measurements at dry (Gas saturated) and wet (100% water saturated) conditions



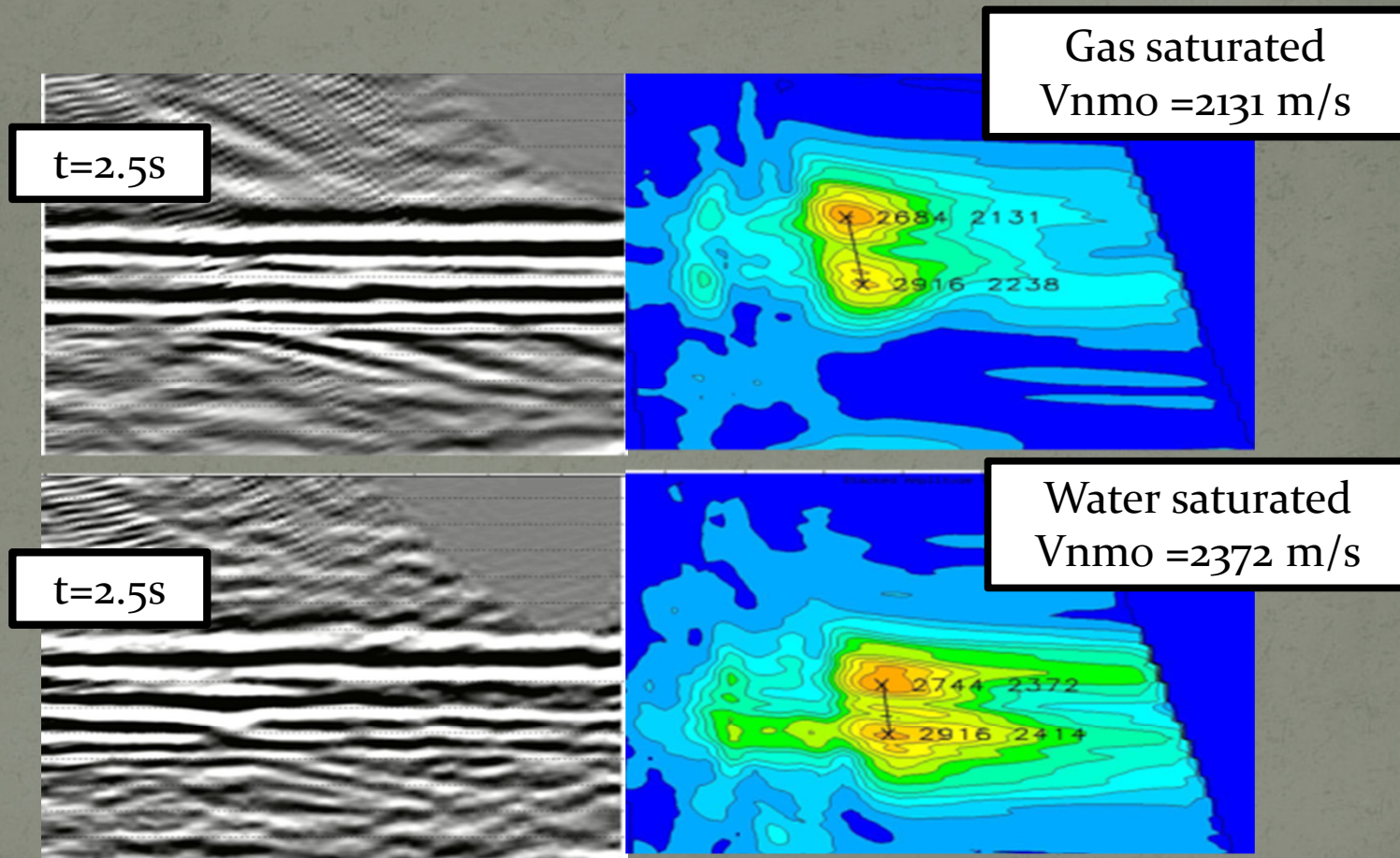
Azimuthal NMO analysis

Min offset = 400m, Max offset = 2200m, Offset interval = 30m



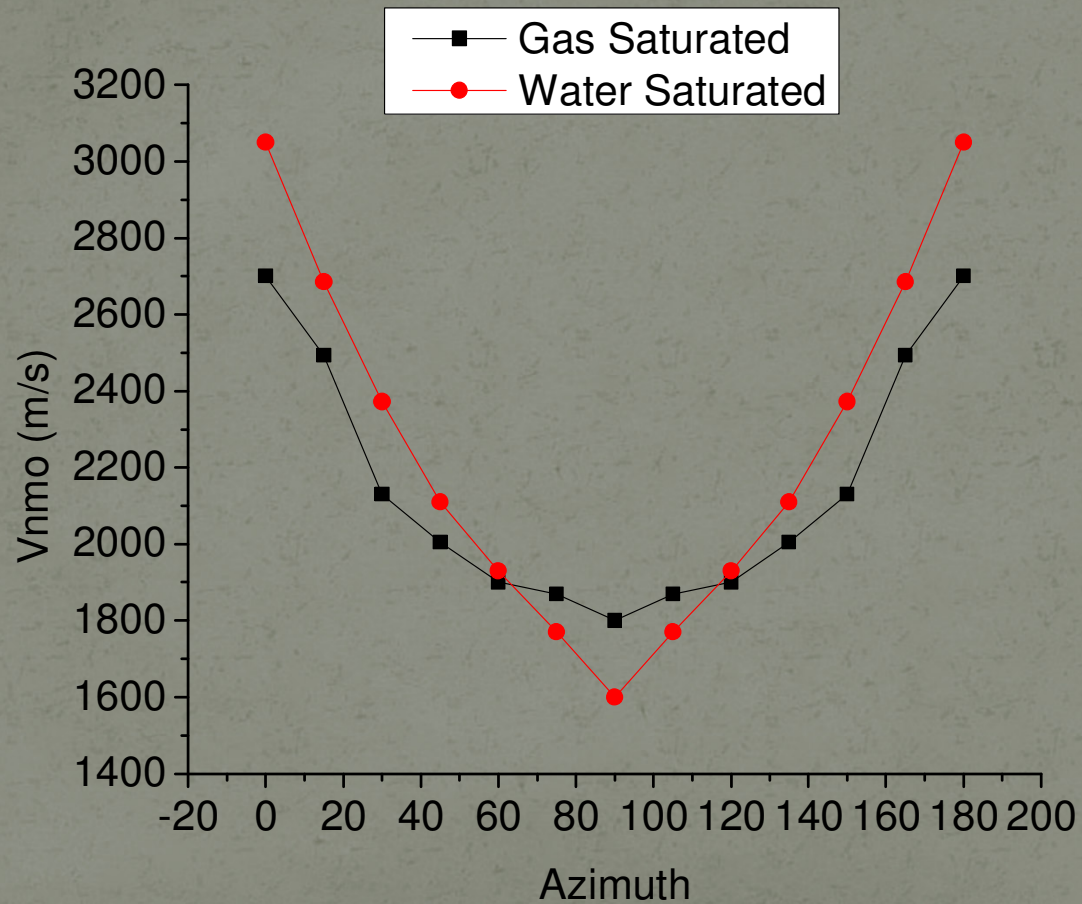
All travel time and distance/offset measurements are scaled by a factor of 10,000

Azimuthal NMO analysis

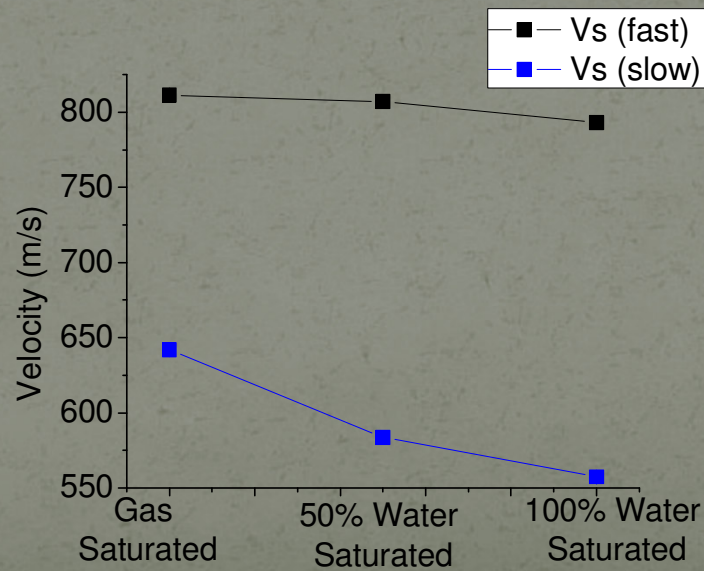
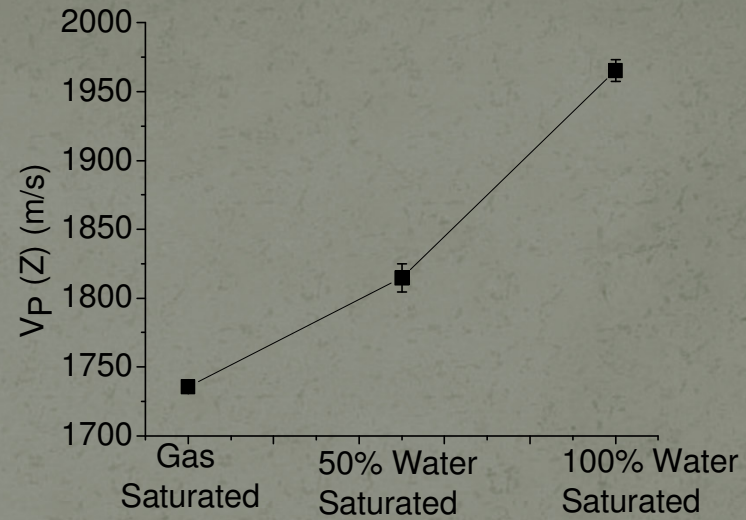
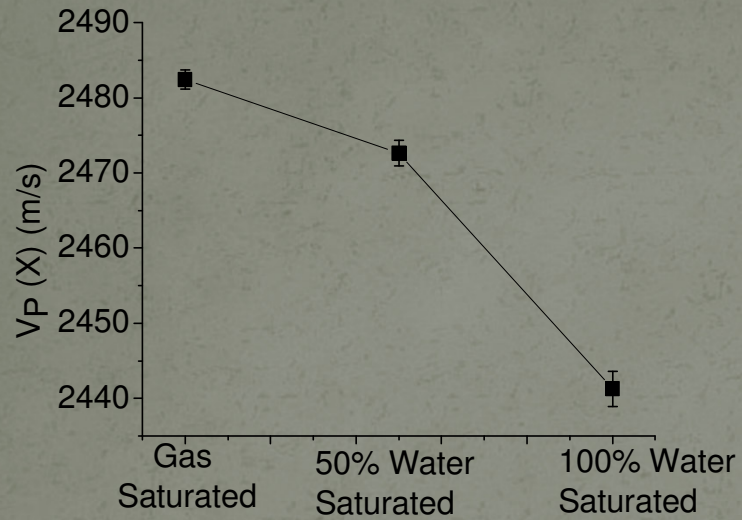


NMO corrected gather at 30° azimuth at gas and water saturated conditions

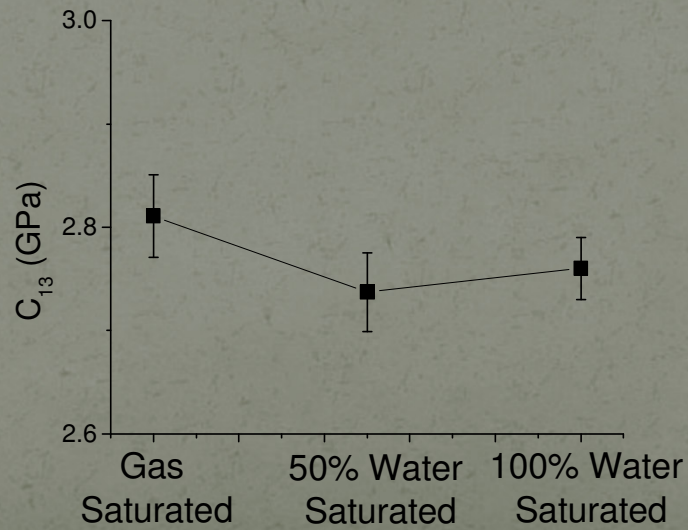
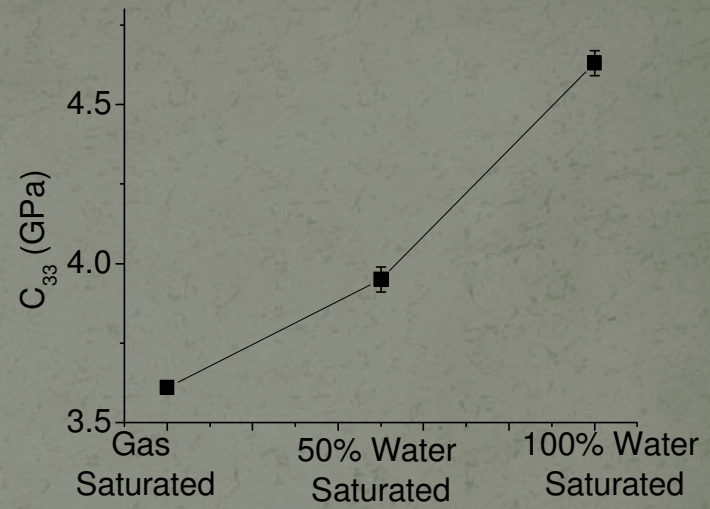
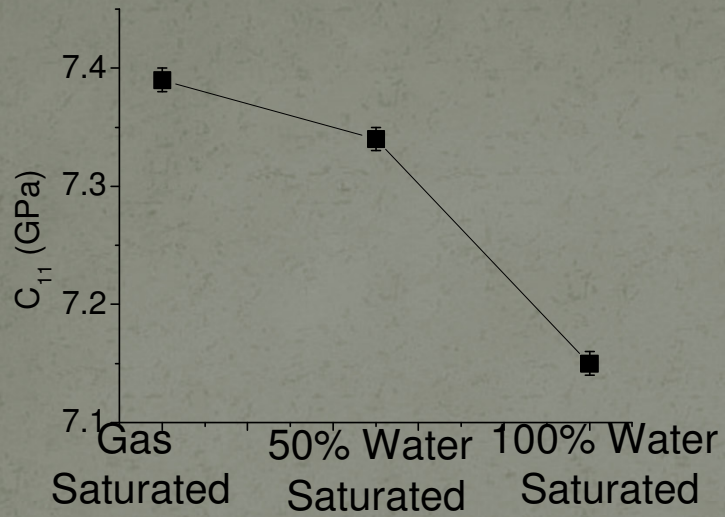
Azimuthal NMO analysis



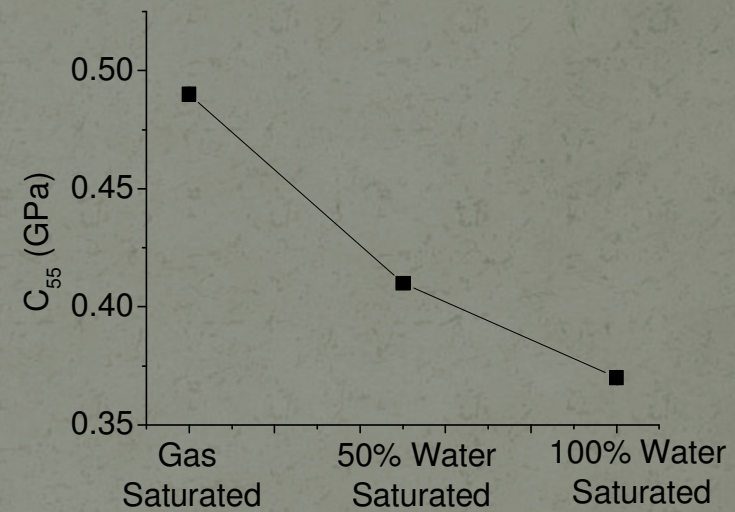
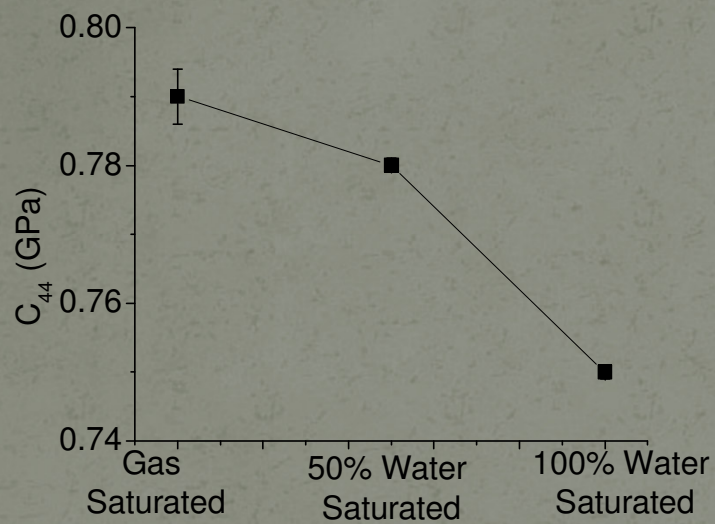
Phase velocities



Stiffness coefficients



Stiffness coefficients



Stiffness coefficients

$$\begin{pmatrix} 7.40 & 2.81 & 2.81 & 0 & 0 & 0 \\ 2.81 & 3.61 & 2.04 & 0 & 0 & 0 \\ 2.81 & 2.04 & 3.61 & 0 & 0 & 0 \\ 0 & 0 & 0 & 0.79 & 0 & 0 \\ 0 & 0 & 0 & 0 & 0.49 & 0 \\ 0 & 0 & 0 & 0 & 0 & 0.49 \end{pmatrix}$$

GPa Gas Saturated

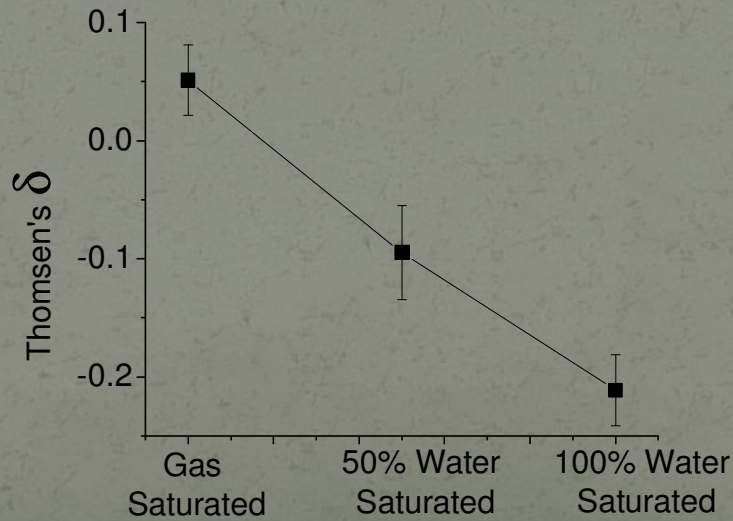
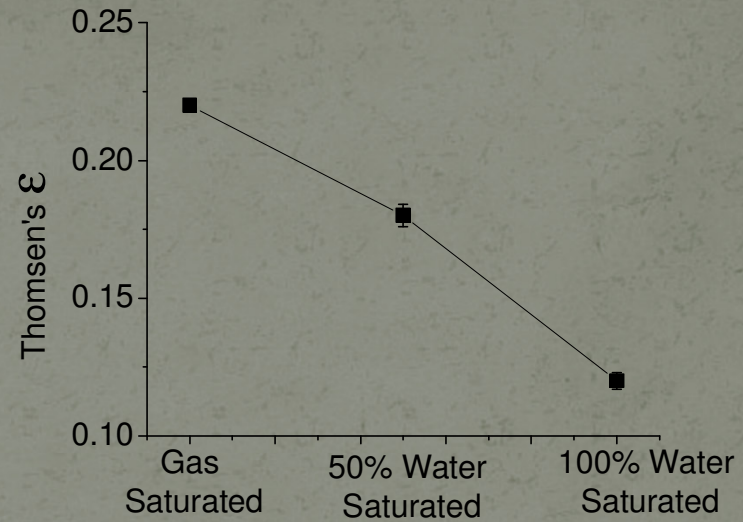
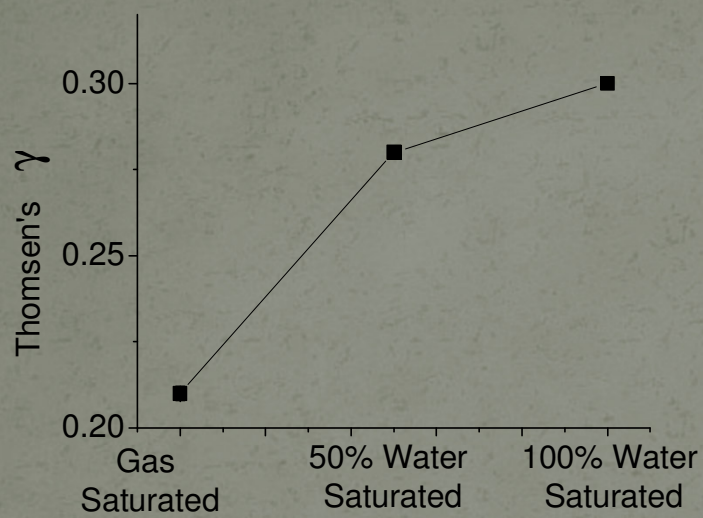
$$\begin{pmatrix} 7.15 & 2.76 & 2.76 & 0 & 0 & 0 \\ 2.76 & 4.63 & 3.89 & 0 & 0 & 0 \\ 2.76 & 3.89 & 4.63 & 0 & 0 & 0 \\ 0 & 0 & 0 & 0.75 & 0 & 0 \\ 0 & 0 & 0 & 0 & 0.37 & 0 \\ 0 & 0 & 0 & 0 & 0 & 0.37 \end{pmatrix}$$

GPa Water Saturated

$$\begin{pmatrix} -3.37 & -1.77 & -1.77 & 0 & 0 & 0 \\ -1.77 & +22 & +47.5 & 0 & 0 & 0 \\ -1.77 & +47.5 & +22 & 0 & 0 & 0 \\ 0 & 0 & 0 & -5.06 & 0 & 0 \\ 0 & 0 & 0 & 0 & -24.4 & 0 \\ 0 & 0 & 0 & 0 & 0 & -24.4 \end{pmatrix}$$

Percentage difference from gas to water saturated conditions

Anisotropic parameters



Conclusion/Future Work

- Experimental results show that shear wave splitting is affected by the nature of the saturating fluid.
 - Results show a 45% decrease in ε and 30% increase in Υ as a function of water saturation.
 - NMO velocities shows different trends with source-receiver azimuth as a function of water saturation.
 - Stiffness coefficients C_{33} and C_{55} are most affected by change in the saturating fluid.
-
- Repeat experiment with a different saturating fluid (glycerin)
 - Quantitative AVAZ analysis on CMP gathers
 - Anisotropic reflectivity modeling from computed stiffness coefficients

References

- Ebrom, D. A., R. H. Tatham, K. K. Sekharan, J. A. McDonald, and G. H. F. Gardner, 1990, Hyperbolic travelttime analysis of first arrivals in an azimuthally anisotropic medium: A physical modeling study: *Geophysics*, 55, 185–191.
- Ebrom, D., J.A. McDonald, 1994, Seismic physical modeling: *Geophysics Reprint Series*
- Hudson, J. A., 1981, Wave speeds and attenuation of elastic waves in material containing cracks. *Geophysical Journal of the Royal Astronomical Society*, 64, 133–150.
- Hudson, J. A., T. Pointer, and E. Liu, 2001, Effective-medium theories for fluid-saturated materials with aligned cracks. *Geophysical Prospecting*, 49, 509–522.
- Omoboya, B., J. J. S, de Fegueiredo., N, Dyaur., and R. R, Stewart., 2011, Uniaxial stress and ultrasonic anisotropy in a layered orthorhombic medium. *SEG Expanded Abstracts* 30, 2145-2149
- Thomsen, L.,1986, Weak elastic anisotropy *Geophysics*, 51, 1954-1966.
- Thomsen, L., 1995, Elastic anisotropy due to aligned cracks in porous rock₁. *Geophysical Prospecting*, 43, 805–829.
- Tsvankin, I., 1997, Reflection moveout and parameter estimation for horizontal transverse isotropy. *Geophysics* 62, 614-629.